Methods for probing the long range dynamic of confined polymer in nanoparticles using small angles neutrons scattering

Yahya Rharbi, Mohamed Yousfi, Lionel Porcar, Qamar Nawaz

Methods for probing the long-range dynamic of confined polymers in nanoparticles using small-angle neutron scattering

Y. Rharbi, M. Yousfi, Lionel Porcar, and Q. Nawaz

Abstract: Motivated by the recent advances in new technologies, a lot of effort has been dedicated to developing methods for quantifying the dynamic of nanoconfined polymers. Particularly, polymers confined in nanoparticles are an important system for several environment-friendly applications such as waterborne coatings and nanoblends. In this work, we discuss two methods to probe the large scale dynamic of nanoconfined polymers in nanoparticles in two situations: (*i*) nanoblends and (*ii*) the close-packed structure. In the methods we apply stress at the nanoscopic level around the polystyrene particles and we probe their deformation in real time using small-angle neutron scattering. These methods give new possibilities to probe, in a nonintrusive manner, the dynamic of confined polymers in nanoparticles, which could ultimately bring conclusive insight to this field.

Key words: polymer dynamic, confinement, nanoblends, polymer nanoparticles.

Résumé : Motivés par les développements récents dans les nouvelles technologies, beaucoup d'efforts ont été déployés dans le but de mettre au point des méthodes permettant de quantifier la dynamique des polymères nanoconfinés. En particulier, les polymères confinés dans des nanoparticules sont des systèmes importants pour plusieurs applications respectueuses de l'environnement, tels les enduits et les mélanges aqueux. Dans ce travail, on discute de deux méthodes d'étudier la dynamique à grande échelle des polymères nanoconfinés dans des nanoparticules, dans deux situations: (*i*) les nanomélanges et (*ii*) la structure à grande compacité. Dans ces méthodes, on applique un stress au niveau nanoscopique autour des particules de polystyrène et on étudie leur déformation en temps réel en faisant appel à la diffusion des neutrons à angles faibles. Ces méthodes fournissent de nouvelles possibilités pour étudier, d'une façon non intrusive, la dynamique des polymères confinés dans des nanoparticules et elles pourraient éventuellement permettre d'obtenir un éclairage conclusif pour comprendre ce champ.

Mots-clés : dynamique des polymères, confinement, nanomélanges, nanoparticules de polymère.

[Traduit par la Rédaction]

Introduction

There are numerous indications that the dynamic of nanoconfined polymers near an interface deviates from that of the bulk.[1–23] This property is of great importance for several nano-technological applications such as the elaboration and stability of nanoscale polymer structures, adhesion, and environment-friendly coatings, among others. By far, thin film is the most studied nanoconfinement geometry[1–19] compared to the other geometries: nanospheres[20–23] and nanotubes.[9] Numerous studies determined the existence of an impressive depression of the nanoconfined glass transition temperature (T_g) in supported and free-standing polystyrene (PS) thin films.[1–6] For supported films, the T_g was found to increase or decrease depending on the nature of the substrate and the polymer.[1,2]

The glass transition temperature in bulk polymers is usually linked to the segmental dynamic, thus, one expects the activation of the dynamic to accompany the observed T_g reduction in confined systems.[1] Therefore, several methods were proposed to monitor the dynamic of confined polymers at different length scales.[7–19] The segmental dynamic in free-standing PS films measured by means of dielectric relaxation was found to be faster than the bulk, which is coherent with the T_g reduction.[7,8] On the other hand, the numerous methods used to probe the large scale dynamic yielded different conclusions. For example, Reiter et al.[10] used the dynamic of dewetting of polystyrene on a solid substrate to extract information on the dynamics of polymer chains. Roth and Dutcher[11] investigated the dynamic of thin films using hole-opening experiments. Russell and co-workers[12] used fluorescence recovery after photobleaching to measure the chain

Received 20 September 2009. Accepted 14 December 2009. Published on the NRC Research Press Web site at canjchem.nrc.ca on 25 February 2010.

This article is part of a Special Issue dedicated to Professor M. A. Winnik.

Y. Rharbi,[1] M. Yousfi, and Q. Nawaz. Laboratoire de Rhéologie, UJF/INPG/CNRS, BP 53, Domaine universitaire 38041, Grenoble, France.
L. Porcar. Institut Laué-Langevin, BP 156 38042, Grenoble, France.

[1]Corresponding author (e-mail: rharbi@ujf-grenoble.fr).

diffusion in polystyrene thin films and found a reduction of the diffusion coefficient with decreasing film thickness. They concluded that chain adsorption on the substrate is what slows chain diffusion. O'Connell and McKenna[13] carried out mechanical tests using the "bubble inflation" technique on ultrathin films and suggested a strong reduction of rubbery compliance as the film thickness decreases, which could mean a higher entanglement density than in the bulk. Bodiguel and Fretigny[14] monitored the dynamic of contraction in free-standing thin films under the action of surface tension and did not find any variation of the rubbery plateau. However, they reported a reduction of the viscosity with decreasing film thickness.[14] Si et al.[15] performed stretching experiments on free-standing films and proposed that intrachain entanglement decreases with decreasing film thickness. Recently, several researchers investigated the dynamics of the free surface layer of polystyrene films by looking at the time dependence of hole closure.[16–19] Reference 16 suggested that the relaxation of the free surface exhibits a bulk behavior for temperatures close to the bulk T_g and then strongly deviates from the bulk relaxation for temperatures below the T_g. To explain the discrepancy between the results of the literature there is still a need to develop new methods to precisely probe the dynamic of confined polymers.

The confinement of polymers in nanoparticles is important in many environmental applications:[20,21] blends, copolymers, nanocomposites, colloids, coatings, and so forth. One example is zero volatile organic compound (VOC) coatings, where polymer nanoparticles are used in the film-making process.[22–26] VOCs are used in coatings to lower the particle T_g and to soften the particle, which permits the fabrication of crack-free films at room temperature.[20,21] If the polymer dynamic is activated and the T_g decreases by decreasing the nanoparticle size, the use of VOCs could be avoided, which would have a positive impact on the environment. Another example is in nanoblends, where hard polymer nanoparticles are used to reinforce soft matrices. If confinement in this application causes the reduction of the hard particles' T_g and the activation of the polymer dynamics, reducing the particle size would be counterproductive for reinforcement since it would cause the softening of the hard particles.[27,28] Thus, there is a real need to develop appropriate methods to measure the dynamics of polymer in nanoparticles.

In this paper, we discuss two methods to monitor the large scale dynamic of polystyrene in nanoparticles in two situations: polymer particles in nanoblends and polymer particles in a close-packed structure. We apply stress to the particles at the nanoscopic level using various procedures and we probe the deformation of the particle in real time by means of small-angle neutron scattering. Particle deformation is then used to quantify the dynamic of confined polystyrene in nanoparticles. Recently, we proposed a method for probing the dynamic of polystyrene nanoparticles in nanoblends[28] and we applied it to a single particle size (80 nm). In the present paper, we first extend these results by discussing the effect of particle. Secondly, we discuss how the void closure between close packed particles could be used to monitor the absolute values of the relaxation time of polymer nanoparticles.

Experimental

Materials

Monomers, deuterated styrene (D_8, Sigma-Aldrich, 99%), nondeuterated styrene (Sigma-Aldrich, 99%), butyl acrylate (Sigma-Aldrich, 99%), butyl methacrylate (Sigma-Aldrich, 99%), and cross-linker, ethylene glycol dimethylacrylate (EGDMA), were used as received. The surfactant, sodium dodecyl sulfate (SDS, Sigma-Aldrich, 99%), the initiator, potassium persulfate (KPS, Sigma-Aldrich, 98%), and buffer sodium bicarbonate were used as received. Double deionized water was used in the emulsion polymerization.

Synthesis

Poly(butyl methacrylate) (PBMA), poly(butyl acrylate) (PBA), deuterated polystyrene (dPS), and hydrogenated polystyrene (PS) particles were prepared using emulsion polymerization at 80 °C. The polymer concentrations in water were 10 wt% for the PBMA, 10 wt% PS, and 2 wt% for dPS. The PBMA particles were cross-linked at 10% using ethylene glycol dimethylacrylate (EGDMA) during the polymerization. The PBMA and PS nanoparticles were prepared in a standard three-neck round flask (500 mL) with a condenser and a nitrogen inlet. For the preparation of PBMA, the mixture (26 g) of the cross-linker (EGDMA) and monomer (BMA) were added to the predegassed SDS (3 g)/water (250 g) solution, which had previously been heated at 80 °C. The solution was vigorously agitated for 20 min before the initiator was added. A solution of the initiator KPS (33 mg) in water (1.7 g) was added to the reaction. After 4 h, another solution of the KPS (5.4 mg) in water (0.7 g) was added to polymerize all the nonreacted styrene monomer.

The dPS was either prepared from pure deuterated styrene (D_8) or from a 50/50 wt% mixture of deutertaed styrene (D_8) and hydrogenated styrene. The dPS particles were prepared in a 50 mL minireactor equipped with a gas inlet and a homemade minicondenser. The size of the dPS particles was controlled by varying the added amount of surfactant in the reaction. The mixture of water (18 g) and SDS was heated to 80 °C, under nitrogen flux for 20 min and then 0.3 g of styrene monomer (50/50 wt% deuterated and hydrogenated) was added. A solution of the initiator KPS (14 mg) in water (0.5 g) was added to the reaction. After 4 h, another solution of the KPS (1.4 mg) in water (0.25 g) was added to polymerize all the nonreacted styrene monomer. The SDS concentration was varied to control the size of the particles.

The surfactant and free ions were removed from the dispersions using a mixture of anionic and cationic exchange resins (Dowex, Sigma-Aldrich). The suspensions were cleaned a few minutes prior to film preparation.

Polymer and particle characterization

Particle diameters (D) were measured using quasi elastic light scattering (QELS) (Malvern 5000) at a 90° angle. The molecular weight was measured using gas permeation chromatography (GPC) in tetrahydrofuran (THF). The molecular weight of PS-93 was found to be $M_w \approx 280\,000$ kg/mol and its $M_n \approx 92\,000$ kg/mol. For dPS-5 the $M_w = 371\,000$ kg/mol and the $M_n = 216\,000$ kg/mol.

The bulk glass transition temperature of polystyrene was measured by differential scanning calorimetry (DSC, Mettler

Table. 1. Properties of the PBMA and PS samples.

	PBMA-10	PBA-10	dPS-5	dPS-6	dPS-1	PS-93
Cross-linking percentage	10%	10%	0%	0%	0%	0%
Particle diameter (nm)	55	50	80	77	30	93
T_g (°C)	55		103	103	99	104.4

Toledo DSC 823) during the heating step at a rate of 10 K/min for polystyrene and 40 K/min for highly cross-linked PBMA. The powder dried at 45 °C, was added to the DSC pan, and annealed for 10 min at 140 °C to remove the thermal history before the first DSC scan. The T_g is taken as the midpoint in the DSC trace, and in Table 1, we report the T_g value from the first run. Also in Table 1, we list the properties of dPS and cross-linked PBMA.

Preparation of the samples for the neutron scattering

The surfactant and free ions were removed from the dispersions using a mixture of anionic and cationic exchange resins (Dowex, Sigma-Aldrich). The dPS-5 suspension was annealed in a stainless steel bomb at 120 °C for 20 min to release their thermal histories.

The nanoblends were prepared by mixing dPS and PBMA dispersions to make dPS concentrations of 2 wt% of the solid PBMA. The blends containing dPS-1 and dPS-6 were prepared using PBMA (lot 2) and dPS-5 was prepared from a PBMA (lot 1). Cracked films were obtained after water evaporation at 56 °C. The hydrogenated PS samples were prepared by drying the PS suspension at 45 °C for 48 h. This yielded a cracked PS powder.

SANS experiments

The small-angle neutron scattering (SANS) experiments were carried out on spectrometer PAXY of Laboratoire Léon Brillouin (LLB, Saclay, France) at the reactor Orphée Saclay and at D22 and D11 of Institut Laué-Langevin (ILL, Grenoble, France). The scattered neutrons, collected on an XY bidimensional multidetector, were circularly averaged to obtain spectra of intensities (I) versus the magnitude of the scattering wave vector (Q). Several configurations of the wavelengths and sample-to-detector distances were chosen to yield a range of Q values between 2×10^{-3} and 1×10^{-1} Å^{-1}.

The nanoblend samples were prepared by gently grinding the cracked films into a powder with grains of 0.5 mm beads. This powder (105 mg) was then introduced between two quartz disks separated by a spacer of 12 mm inner diameter and 1.2 mm thickness. The nanoblends were annealed (in situ), the sample was positioned in the neutron beam in a homemade oven equipped with two quartz windows and was heated to the desired temperature during the SANS measurements. The sample temperatures were monitored using a thin thermocouple placed in the proximity of the sample. The sample temperature was found to reach the desired temperature within 2 min. Neutron spectra were taken for 1 min at various annealing times.

The PS samples were separated into several samples of 0.2 g placed in glass bottles. Each of these samples were annealed at 100 °C ± 0.2 °C for a given time between 1 min and 2 h. The samples were then gently grinded into 0.5 mm beads. This powder (0.09 ± 0.002 g) was then placed between two pieces of aluminum scotch tape (0.1 mm thick) separated by a spacer of 14 mm inner diameter and 0.8 mm thickness. The powder was then pressed using 15 kgf/cm^2 (1 kgf/cm^2 = 98.0665 kPa) to obtain a homogeneous film thickness of 0.8 mm.

Results and discussion

A good protocol to monitor the dynamic of polymer nanoparticles requires (*i*) that a stress is applied to the particle at the nanoscopic level and (*ii*) a sensitive method to monitor the change in the particle shape during its deformation. From the time dependence of the particle shape one can deduce the relaxation time of the polymer and its dependence on the temperature and the confinement condition. We apply this procedure to probe the dynamic of polystyrene in two different environments: (*i*) polystyrene dispersed in nanoblends and (*ii*) close-packed polystyrene particles.

Protocol for measuring the dynamic of polystyrene nanoparticles in nanoblends

In a previous report, we proposed a new method to apply the stress locally to the polystyrene nanoparticles dispersed in nanoblends by using the following procedure:[28] Nanoblends composed of colloidal suspensions of cross-linked PBMA and 2% dPS nanoparticles were prepared via water evaporation, see Scheme 1. These blends were prepared at temperatures above the T_g of cross-linked PBMA particles (T_g^{PBMA}) and well below the T_g of PS (T_g^{PS}). This should lead to a deformation of the PBMA particles under capillary pressure ($P_{Lap} = 12.9\gamma_{aw}/R \sim 23$ MPa, where γ_{aw} is the surface tension of air/water and R is the radius of the particle) filling the voids between them while the glassy dPS nanoparticles remain spherical. With $P_{Lap} \sim 23$ MPa, the glassy PS particles with a modulus $G \sim$ GPa should remain spherical at the temperature of film formation (T^f). The cross-linked PBMA particles, which exhibit an elastic modulus of $G < 23$ MPa are expected to deform under $P_{Lap} \sim 23$ MPa for $T^f > T_g^{PBMA}$. This leads to storage of elastic energy within the PBMA nanoparticles.

After annealing the nanoblends above the T_g^{PS}, the PBMA around the PS release the stored elastic energy by partially regaining their spherical shape, which induces the deformation of the PS particles (Scheme 1). SANS is then used to monitor the evolution of the shape of the PS particle and to quantify the dynamic of the confined polystyrene.

The adequate procedure to obtain individual nanoparticles in nanoblends

To properly study the confined PS in nanoblends, one should first succeed in making films containing PS particles individually dispersed within cross-linked matrices. When the PS and the matrix-forming particles are mixed at low concentrations, they remain stable in water because of electrostatic repulsion. The idealistic situation to obtain a con-

Scheme 1. Description of the procedure for measuring the dynamic of PS in nanoblends. Step 1 is the procedure of nanoblends preparation and step 2 is the procedure for annealing the nanoblends (reproduced from ref. 28).

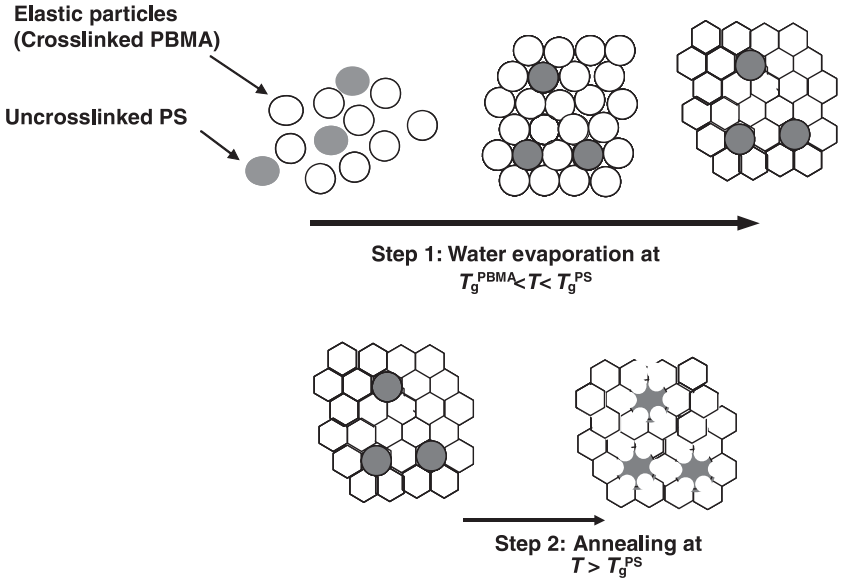

trolled dispersion at the nanoscopic level is that the two particles remain stable throughout the whole water evaporation process. During water evaporation the particle concentration increases, which could affect the stability of the different particles.

In Fig. 1, we compare the SANS spectra of 30 nm dPS particles dispersed in PBA and PBMA matrices. The spectra of dPS in a PBA matrix exhibit a strong scattering for $q \rightarrow 0$, which could be fitted to a power law with an exponent of –2.85. This suggests that dPS particles form large aggregates of dPS particles in the PBA matrix. On the other hand, the spectra of the same dPS particles in PBMA yields a low scattering intensity for $q \rightarrow 0$, which suggests that dPS are individually dispersed within the PBMA matrix. As we showed before when the PS and PBMA suspensions are cleaned using the ion exchange procedure, one can obtain nanoblends with perfect dispersion of the PS in the PBMA.[27] On the other hand, we could not obtain individual PS particles in the PBA even when both suspensions are cleaned in the same procedure as in the PS/PBMA. This shows that the ability to obtain nonaggregated particles in the blends depends on the physicochemical properties of the two particles during evaporation. In the following, we focus our discussion on the nanoblends of dPS in the PBMA matrix.

The SANS spectra of blends containing 2 wt% dPS (30, 77, and 80 nm) dispersed in a 10% cross-linked PBMA matrix exhibit a continuously decreasing scattering intensity, $I(q)$ (Fig. 2). The $I(q)$ were found to fit well to the $P(q)$ of polydispersed hard spheres (Fig. 2). The best fit was found to yield for dPS-6 (77 nm) a mean particle diameter of 73 nm and for the dPS-1 (30 nm) a particle diameter of 28 nm. These diameters are similar to those from quasi elastic light scattering. This infers that the dPS nanoparticles are individually dispersed within the PBMA matrices and remain spherical in the blends. The intensity, $I(q)$, can be written as $I(q) = P(q) \cdot S(q)$ where $P(q)$ is the form factor and $S(q)$ is the structure factor of the dPS particles. $S(q) \approx 1$

Fig. 1. SANS spectra of films made from 2 wt% deuterated polystyrene particles (30 nm) dispersed in a 10% cross-linked PBA matrix (■) and in 10% cross-linked PBMA matrix (□). The films were prepared via evaporation at 56 °C of a mixture of dPS/PBMA (■) and dPS/PBA (□) suspensions.

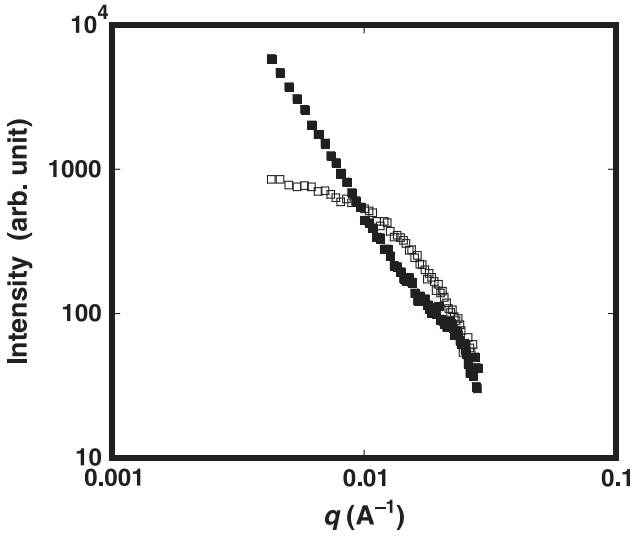

because of a low dPS concentration and the absence of selective aggregation. The spectra in Fig. 2 also imply that the cross-linked PBMA particles are deformed under Laplace pressure to fill the interstices. If not, a strong scattering peak from the PBMA matrix at $q = 2\pi/D_{PBMA} = 0.01$ Å^{-1} would be visible, similar to that observed in glassy PS particles as will be discussed later.

Change of the shape of the particle after annealing

When the nanoblends of 77 nm dPS nanoparticles in 10% cross-linked PBMA are annealed above the bulk T_g, the shape of the dPS particles changes remarkably. The oscillations of the scattering spectra disappear and the intensity, $I(q)$, decreases for $q < 0.01$ Å^{-1} and increases for

Fig. 2. SANS spectra of films made from 2 wt% deuterated polystyrene particles dispersed in a 10% cross-linked PBMA matrix: (a) 77 nm dPS (PS-6) and (b) 30 nm dPS (PS-1) particles. The films were prepared from a mixture of two suspensions: 10% cross-linked PBMA particles (56 nm) and dPS nanoparticles. The films were prepared by evaporation at 56 °C (above the T_g of PBMA and below T_g of dPS). The SANS curves are fitted to a form factor of (a) polydispersed spheres with a diameter of 73 nm and a polydispersity of PDI = 7% and (b) to polydispersed spheres with a diameter of 28 nm. (Insert: SANS of 80 nm particle (dPS-5) for a wide range of q, up to q = 0.1 Å^{-1}, fitted to a factor of spherical particle.)

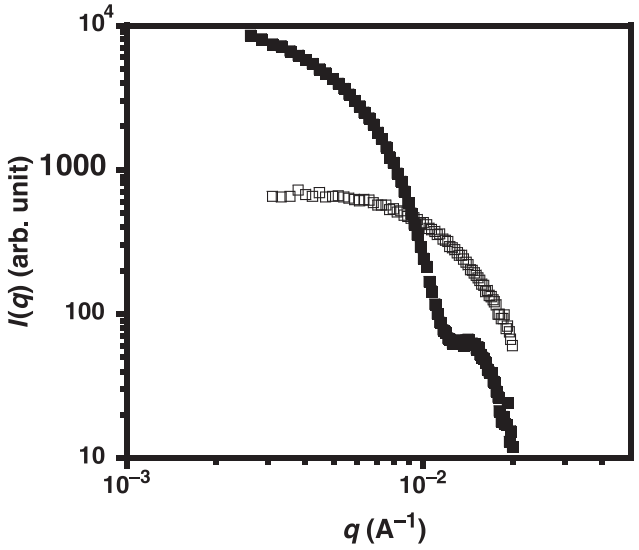

$q > 0.01$ Å^{-1}. This observation is found to be the same as the 80 nm dPS sample (dPS-5) reported previously.[28] The 30 nm particle also clearly shows the decrease of the intensity at q values after annealing. The evolution of the SANS spectra shows that the shape of the dPS nanoparticles evolves during the annealing process. We have shown previously that such change results from a deformation of the individual dPS particles during annealing.[28] One could imagine that the change in the SANS spectra results from penetration of deuterated polystyrene chains in the PBMA matrix or fusion of dPS particles. Fusion is unlikely because it results in large particles with a lower total surface area. This specific interface area between the dPS and the PBMA is estimated using the Porod law as $q^4 \cdot I(q)$ at large q values. The average value of $q^4 \cdot I(q)$ is found to triple after annealing, contrary to what is expected in fusion (Fig. 3 from ref. 28). Furthermore, since fusion yields large particles, a high scattering intensity for $q \rightarrow 0$ is expected ($I(0) \sim \varphi \cdot V_{part}$, where φ is the volume fraction and V_{part} is the volume of the particles). In fact, the measured $I(q)$ for low q after annealing is lower than $I(q)$ of the nonannealed films in the range of q values investigated. This could mean that the volume of dPS particles remain unchanged despite the change in their shape. One could also imagine that the change in the SANS spectra results from penetration of deuterated polystyrene chains in the PBMA matrix. Polystyrene and uncross-linked PBMA form an interface which is a few nanometers thick,[29] whereas highly cross-linked PBMA is likely to inhibit the interpenetration of the polymers. If penetration of dPS into the PBMA matrix is what causes the observed transformation in the SANS spectra, then the change should be more enhanced in low cross-linked PBMA matrices. In contrast with this, the spectra of films made of low cross-linked PBMA matrices remain slightly the same upon annealing (Fig. 4 from ref. 28). It is therefore clear that fusion of dPS nanoparticles and penetration of dPS into the PBMA matrix are not responsible for the observed transformation of the SANS spectra upon annealing. The change of SANS spectra most likely results from the deformation of individual polystyrene nanoparticles, which is dictated by the behavior of the surrounding cross-linked PBMA particles. During annealing, the cross-linked PBMA particles regain their spherical shape and squeeze the dPS particles between them. Such mechanism is likely to produce a dPS nanoparticle with an elongated shape with many branches. The simplest picture is that the dPS nanoparticles deform into a star-like shape with 12 branches according to Scheme 1.

Dynamics of deformation of polystyrene confined in nanoblends at temperatures above the bulk glass transition

The shape of the spectra of 77 nm dPS in a 10% cross-linked PBMA matrix continuously changes during annealing at 140 °C: the intensity at low q decreases and that of large q increases (Fig. 3a). The evolution of the spectra with time reflects the change in the particles' shape during their deformation. Annealing the nanoblends with 30 nm particles at 140 °C gives the same behavior as the 77 nm particles (Fig. 3b): the intensity decreases in the low q range. This shows that this procedure can be used to test the dynamic of dPS particles in nanoblends for particles as small as 30 nm.

To quantify the dynamics of polystyrene particles in nanoblends, we can either use (*i*) the change of the scattering intensity at various q values, $I(q,t)$, or (*ii*) the variation of the gyration radius, R_g, of the dPS particle with time. In Fig. 4a, we show the scattering intensity at various q values for 77 nm dPS particles in 10% cross-linked PBMA matrix annealed at 140 °C. These plots fit perfectly to a stretched exponential with an exponent of $\beta = 0.6$ (Fig. 5) and a relaxation time, τ, which depends on the q value. The reliability of the fit and the estimation of the error bar in β and τ are estimated from the width of the minimum of the least-squares plots versus β and τ. The magnitude of change in the scattering intensity during annealing decreases when one approaches the minimum of $P(q)$, which makes it difficult to monitor the dynamic for $q > 0.005$ Å^{-1} for 77 nm and $q > 0.01$ Å^{-1} for 30 nm particles.

The $R_g(t)$ at various annealing times is calculated by fitting the low q values of $I(q)$ using the Guinier representation, $\ln(I(q)) = \ln(I(0)) - q^2 \cdot R_g^2/3$. The $R_g(t)/R_g(0)$ decay for 77 nm dPS fits perfectly to a stretched exponential with a decay time of $\tau_{Rg} = 25$ min and $\beta = 0.64$ (Fig. 6). This behavior is exactly the same as that found previously on 80 nm particles;[28] however, the exponent was found to be $\beta = 0.716 \pm 3\%$, which is slightly higher than that found here. This infers that the exponent depends slightly on the property of the dPS particle and the surrounding matrix.

Fig. 3. (a) The scattering spectra plotted for various annealing times for 77 nm dPS nanoparticles in a 10% cross-linked PBMA matrix before annealing (□) and at 4 (■), 17 (Δ), and 37 min (▲). (b) The scattering spectra plotted for various annealing times for 30 nm dPS nanoparticles in a 10% cross-linked PBMA matrix. The films were annealed at 140 °C.

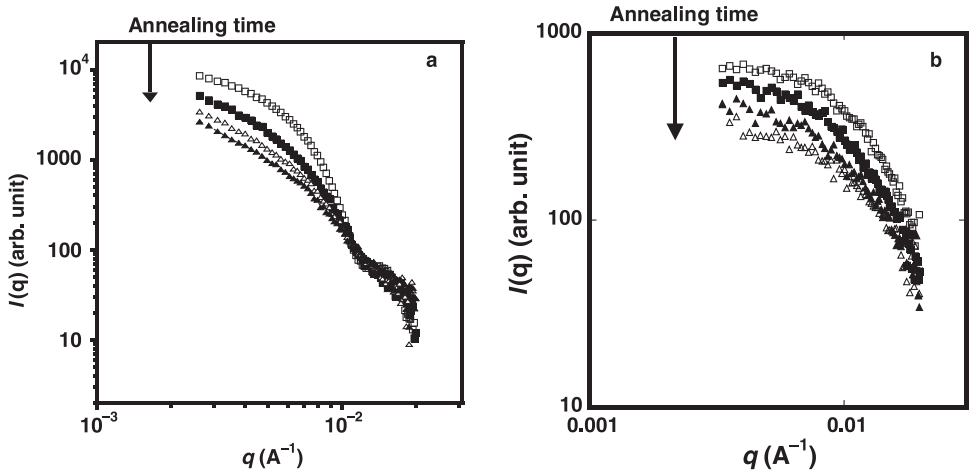

Fig. 4. The evolution of the scattering intensity at various q values, as a function of the annealing time for blends made from (a) 77 nm dPS nanoparticles and (b) 30 nm particles. The plot is fitted to a stretched exponential (continuous lines).

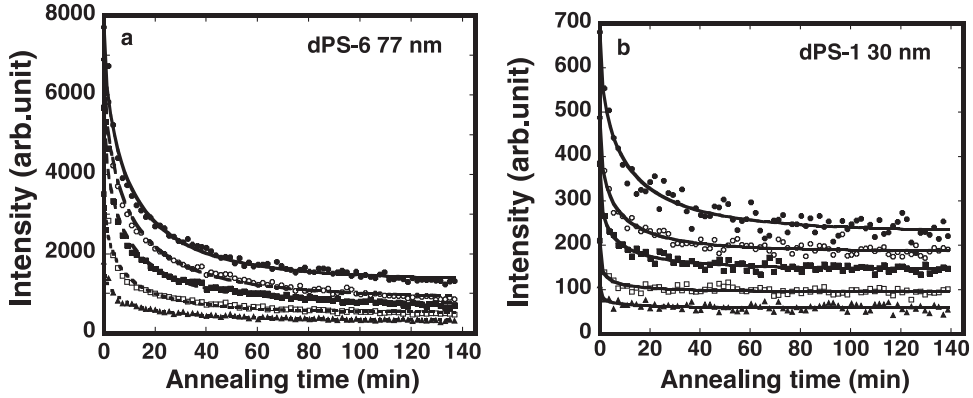

Fig. 5. The exponent β of the fit of the decays ($I(q, t)$) in Fig. 4 to a stretched exponential ($I(q,t) = I(q,0)\exp - (t/\tau)^{\beta}$), plotted against the q values for (a) 30 nm particles and (b) 77 nm particles.

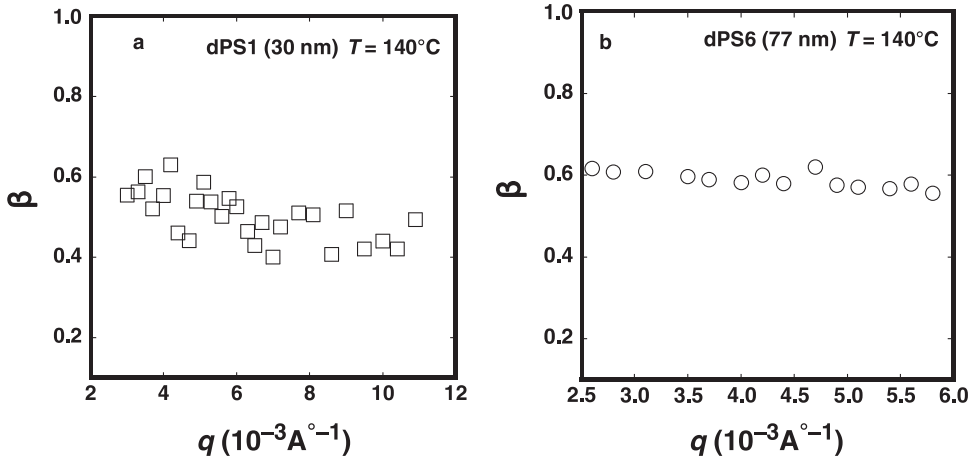

The time decay of the scattering intensity of the 30 nm particle was also found to fit to a stretched exponential with an exponent $\beta = 5$ for $q < 0.01$ Å^{-1}, which is slightly lower than that calculated in large particles (Fig. 5). The relaxation of the bulk PS is well-accepted to be a stretched exponential with an exponent of 0.4.[30] The exponent, β, in our experiment reflects the change in the spreading mechanism of the dPS particle between the PBMA particles and therefore contains information on the exponent of the polymer relaxation as well as other parameters such as the particle size.

Fig. 6. $R_g(t)$ vs. the annealing time for blends made from 77 nm dPS nanoparticles in 10% cross-linked PBMA annealed at 140 °C. R_g is calculated using the Guinier representation.

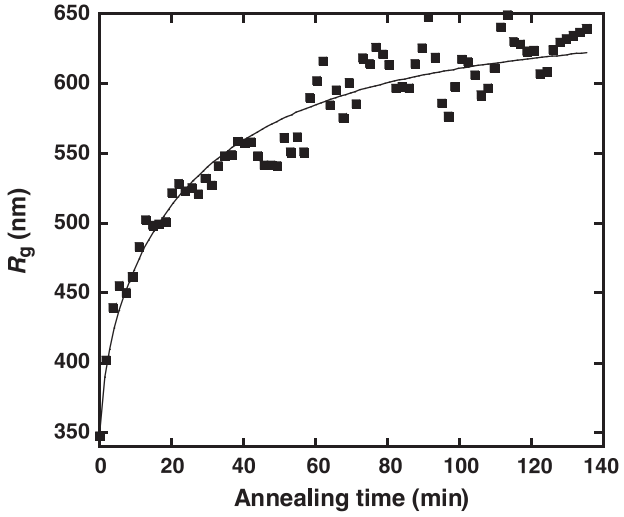

The appropriate parameter to characterize the stretched exponential dynamic is the average relaxation time, $<\tau>$, which is calculated as $<\tau> = \int \exp(-(t/\tau)^{\beta})dt$ using the τ and β values.[31] The $<\tau(q)>$ in 77 nm dPS particles decreases with increasing q from 16.6 min to 11.4 min for q values between 2.58×10^{-3} Å^{-1} and 5.1×10^{-3} Å^{-1} (Fig. 7a). For 30 nm dPS $<\tau>$ was also found to decrease with increasing q in the same manner as the 77 nm particles (Fig. 7b). Such tendency is similar to that reported previously on dPS-6. Since $I(q)$ at each q value portrays the density fluctuations with a size of $\xi = 2\pi/q$, $<\tau(q)>$ also describes the relaxation dynamic of the density fluctuation with a size of ξ. Larger fluctuations would require more time to change than a smaller fluctuation. Therefore, $<\tau(q)>$ increases with increasing ξ and thus increases with deceasing q. For q approaching $q = 0$, $<\tau(q)>$ converges toward the relaxation time of the gyration radius, $<\tau_{R_g}>$, which is the largest size of the system, $<\tau(q)>_{R_g} = 34$ min.

The $<\tau(q)>$ of 30 nm particles is found to be larger than the $<\tau(q)>$ of 77 nm when measured at the same q values (Fig. 7b). The $<\tau(q)>$ and $<\tau_{R_g}>$ describe the dynamic of particle deformation under the applied stress, $\sigma(t)$, and depends directly on the relaxation time of the confined polymer (τ_α). During the film formation, PBMA particles around smaller dPS particles undergo a small deformation as compared to around large particles, thus, they store less stress. Therefore, one expects smaller particles to deform more slowly than large ones if the PS behaves dynamically in the same manner in the two particles. To derive τ_α from $<\tau(q)>$ and $<\tau_{R_g}>$, we assume the polymer to exhibit a single exponential relaxation with a time τ_α and use the following differential equation (eq. [1]).

$$[1] \qquad \frac{d\sigma(t)}{dt} + \frac{\sigma(t)}{\tau_\alpha} = G\frac{d\varepsilon(t)}{dt}$$

where G is the high shear modulus and the deformation strain, $(\varepsilon(t))$, defined by $R_g(t)/R_g(0)$ or $I(q,t)/I(q,0)$. Equation [1] applies only if the time and the position dependence of $\varepsilon(t)$ and $\sigma(t)$ can be separated. It is easy to accept that the stored strain, $\sigma(t)$, decrease with increasing the time in the same manner as $\varepsilon(t)$. If we take $\varepsilon(t)$ and $\sigma(t)$ as exponential with relaxation time, $<\tau(q)>$ or $<\tau_{R_g}>$, we found

$$[2] \qquad \langle\tau\rangle \approx \frac{G}{\sigma(0)}\tau_\alpha$$

The PBMA particles around small dPS particles undergo a small deformation compared to around large dPS ones. Thus, one expects the stored stress, $\sigma(0)$, in the case of small dPS particles to be lower than that in large ones. If we take $\sigma(0)$ to be proportional to the dPS particle diameter, D ($\sigma(0) \propto D$), we found $\tau_\alpha \propto <\tau> \cdot D$. In Fig. 8, we compare the plots $<\tau> \cdot D$ versus q for 77 nm and 30 nm dPS particles. The $<\tau> \cdot D$ of 30 nm particles is found to be lower than that of 77 nm, which could infer that the relaxation time of confined polystyrene, τ_α, of 30 nm is smaller than that of 77 nm.

The decay times, $<\tau(q)>$ and $<\tau_{R_g}>$, contain useful information about the relaxation time of the confined polystyrene in the nanoparticles in nanoblends. The evolution of these times with temperature and the particle size will be used to obtain information on the effect of confinement on the polymer dynamic.

Protocol for measuring the dynamic of polystyrene nanoparticles in a close-packed structure

To apply the stress locally to polymer nanoparticles, we also propose the following procedure: When suspensions of polymer particles are evaporated below the glass transition temperature (T_g) of the polymer, the particles remain spherical and form a close-packed structure separated with voids (Scheme 2, stage II). The presence of a large interface area (polymer/air) in the voids makes the particles a confined system, which could affect the polymer dynamic and, consequently, the kinetic of particle deformation and void closure. The presence of the voids applies Laplace pressure in the interstices due to the air/polystyrene surface tension ($\gamma_{p/a}$), $P_{Lap} = \alpha\gamma_{p/a}/R$, $\gamma_{p/a} = 0.03$ N/m^2. This tends to deform the particle and close the voids to yield a bulk-like polymer (Scheme 2, stage III). If the particles are glassy, the voids should remain unaffected by Laplace pressure during the time of the experiment, and when the system is annealed above the polymer T_g, the particles deform and the voids close. If one can probe the closure of the interstices, then this can be used as a nonintrusive method to study the dynamic of confined polymers in nanoparticles. We used the small-angle neutron scattering technique to probe the deformation of the particles during annealing. Previous experiments used atomic force microscopy to monitor the change in the free surface corrugation during annealing of submicron size particles.[32–35] The dynamic of free surface corrugation in polyacrylate was found to be similar to the bulk dynamic.[34,35]

The SANS spectra of films made from 93 nm PS particles at 45 °C before annealing exhibit a well-defined narrow first peak followed by two small peaks (Fig. 9). The position of the first peak, q^*, corresponds to a characteristic distance of $D^* = 2\pi(3/2)^{1/2}/q^* = 99$ nm, which is almost equal to the hydrodynamic diameter of the particles measured by dynamic light scattering. It is well-accepted that the drying of

Fig. 7. (a) Average relaxation time, $<\tau(q)>$, plotted against q for blends of 77 nm dPS particles in 10% cross-linked PBMA matrix. $<\tau(q)>$ is calculated from the fit of the scattering intensities ($I(q)$ vs. time) to a stretched exponential (Fig. 4). (b) Comparison of the plots $<\tau(q)>$ vs. q of the 77 nm (dPS-6) (■) and 30 nm dPS-1 (□) particles. $<\tau(q)>$ is calculated from the fit of the scattering intensities ($I(q,t)$) to a stretched exponential.

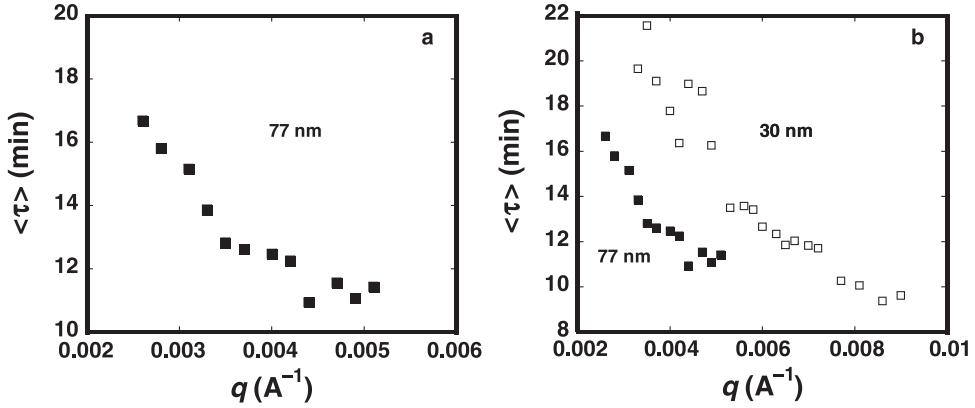

Fig. 8. Relaxation time, $<\tau(q)> \cdot D$ plotted against q for 77 nm (dPS-6) (■) and 30 nm dPS-1 (□). $<\tau(q)>$ is calculated from the fit of the scattering intensities ($I(q)$ vs. time) to a stretched exponential.

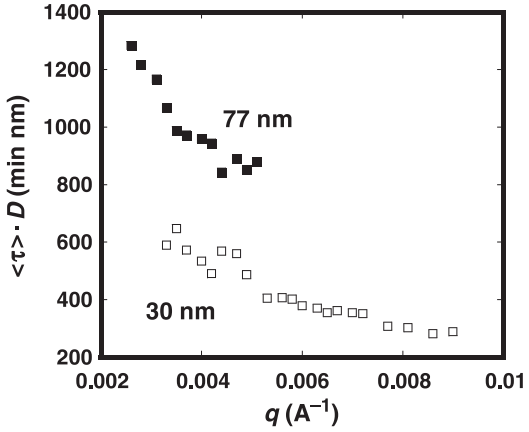

suspensions of monodispersed particles form a face centered cubic structure (FCC).[25] The contrast in the neutron scattering comes from the difference between the PS in the particles and the voids between them. The strong contrast in the SANS when the suspensions are dried below T_g infers that the particles remain spherical and separated with voids (Scheme 1, stage II).

Dynamic of void closure in 93 nm particles at the bulk T_g

When the PS samples are annealed at 100 °C both the first, second, and the third peaks decrease progressively and broaden during annealing (Fig. 9). After 30 min, the second peak disappears while the first peak turns into a broad maximum, and at 60 min both peaks have disappeared. The intensity measured at the first peak decreases steadily during annealing until it becomes purely the incoherent scattering from the PS (Fig. 10). The steady decrease of the intensity results from the progressive closure of the voids under the action of Laplace pressure. The scattering intensity varies as $I(t) \propto (V_{voids}(t))^2$, where V_{voids} is the volume of the voids between the particles. A random close-packed structure corresponds to a volume fraction of the solid of 0.64 and fraction of the voids of 0.36.[36] Thus, the intensity can be written as $I(t) \propto (V_{voids}(0))^2(0.36 - \varepsilon(t))^2$, where $\varepsilon(t)$ is the deformation strain of the sample and $V_{voids}(0)$ is the initial volume of the voids or $I(t)/\ I(0) \propto ((0.36 - \varepsilon(t))/(0.36 - \varepsilon(0))^2$.

Using a generalized Hertezian model[37,38] for the deformation of particles in a close-packed morphology, and assuming film shrinking occurs in the z direction, the governing equation can be written as eq. [3] when the deformation is averaged over all directions and over the entire film.[36]

$$[3] \qquad \frac{6.69(1-\nu)\gamma_{p/a}}{R} = \int_0^t G(t-t')\frac{d\varepsilon^{3/2}}{dt'}dt'$$

where $G(t)$ is time dependent shear stress, $\gamma_{p/a}$ is the surface tension between the PS and air, ν is the Poisson's ratio of polystyrene ($\nu = 0.33$), and R is the particle radius.

Near T_g and for short times, the compliance of PS is dominated by the glassy relaxation process.[47] If we assume the PS in this condition to exhibit a single relaxation time, $\tau(G(t)$ is an exponential), the t_{close} can be calculated from eq. [3] as the time for which $\varepsilon(t_{close}) = 0.36$ to give eq. [4]:

$$[4] \qquad t_{close} \approx \frac{0.0479\,G}{\gamma_{p/a}} R \cdot \tau$$

where G is the high frequency shear stress ($G \sim 1$ GPa) and R the particle radius. From eq. [4], we can estimate $\tau \approx 37$ s for $D = 93$ nm. When the relaxation time was calculated by numerically resolving eq. [3], using the strain $\varepsilon(t)$ from $I(t)/I(0) \propto ((0.36 - \varepsilon(t))/(0.36 - \varepsilon(0))^2$ we found $\tau \approx 44$ s. The polystyrene dynamic in the glassy regime near the T_g is more likely to be a stretched exponential ($G(t) = \exp(-(t/\tau)^\beta)$) with an exponent $\beta = 0.4$.[30,39] In this case, we estimated the average relaxation time, $<\tau>$ ($<\tau> = \int\exp(-(t/\tau)^\beta)dt$), by numerically resolving eq. [3] with $\varepsilon(t)$ from $I(t)/I(0) \propto ((0.36 - \varepsilon(t))/(0.36 - \varepsilon(0))^2$, which leads to $<\tau> \approx 47$ s. This shows that the various methods for calculating the relaxation time yield similar values.

Contrary to the first method described here, this method gives an absolute value of the relaxation time of the confined polystyrene in nanoparticles. The evolution of $<\tau>$ with a change in temperature and particle size will be used

Scheme 2. The three main steps of the film formation process.

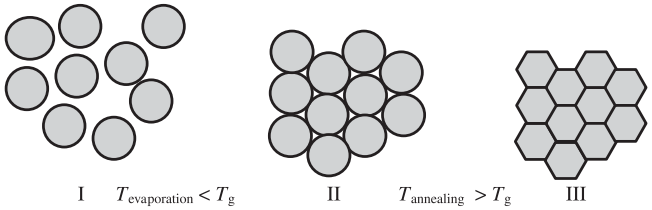

Fig. 9. SANS spectra of film made from 93 nm PS nanoparticles, annealed at 100 °C for various annealing times: 0 (○), 20 (▲), and 60 min (▼).

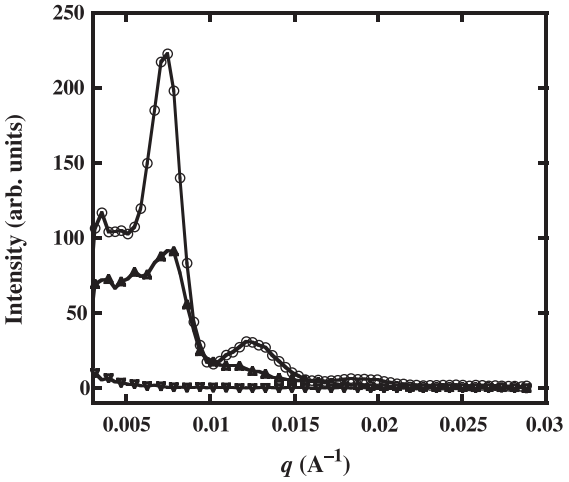

Fig. 10. SANS intensity at the first scattering peak, $I_{max}(t)$, of 93 nm PS particles plotted against the annealing time.

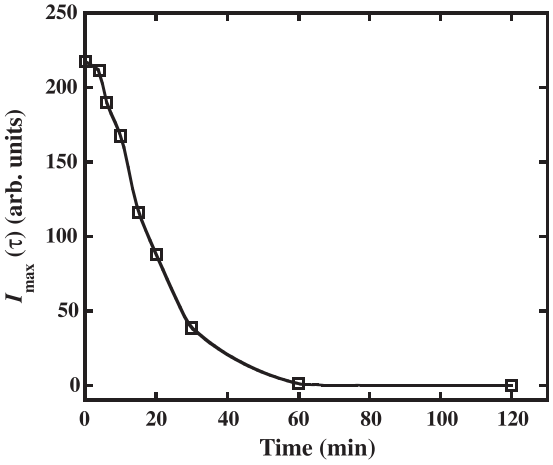

in further work to obtain information on the effect of confinement on the polymer dynamic.

Conclusion

We presented two methods to probe the dynamic of polymers in nanoparticles in two different environments: (*i*) nanoblends and (*ii*) close-packed structures. We use neutron scattering to probe the kinetic of nanoparticle deformation under the action of applied stress at the nanoscopic level. For the nanoblends, we prepared the samples by water evaporation of suspensions of glassy PS and elastic PBMA (cross-linked) nanoparticles at $T_g^{PBMA} < T^{ev} < T_g^{PS}$. This leads to storage of elastic stress in the cross-linked PBMA particles around the PS. During annealing at $T^{annealing} > T_g^{PS}$, the PS particles deform, and this deformation is probed by SANS. The characteristic time from this method can be used to obtain information on the relaxation time of confined PS nanoparticles in nanoblends. In the close-packed structure, the voids between the spherical particles apply Laplace pressure to the particles, which deforms the particle and closes the voids. The kinetic of void closure is used to obtain information on the dynamic of confined PS in nanoparticles. These two methods give new possibilities to probe, in a nonintrusive manner, the dynamic of confined polymers in nanoparticles, which ultimately could bring conclusive insight in this field.

Acknowledgment

We Acknowledge the Pakistani ministry of education, the Higher Education Commission (HEC) of Pakistani and the French Société Française d'Exportation des ressources Éducatives (SFERE) program for Mr. Nawaz's scholarship. We also thank the French ministry of education and the Cluster Matériaux et Conception pour un Developpement durable (MACODEV) program for their financial support. The French neutron facility at the Commissariat à l'Énergie Atomique (CEA) Saclay and the Laboratoire Léon Brillouin (LLB) are gratefully acknowledged for the neutron equipment. We thank Dr. F. Boué (LLB) and Dr. A. Lapp (LLB) for their help in the neutron scattering experiments and for the stimulating discussions. H. Galliard is also acknowledged for her help with these experiments.

References

(1) Alcoutlabi, M.; McKenna, G. B. *J. Phys. Condens. Matter* **2005**, *17* (15), R461. doi:10.1088/0953-8984/17/15/R01.
(2) Forrest, J. A. *Eur. Phys. J. E* **2002**, *8* (2), 261. PMID: 15010978.
(3) Forrest, J. A.; Dalnoki-Veress, K.; Stevens, J. R.; Dutcher, J. R. *Phys. Rev. Lett.* **1996**, *77* (10), 2002. doi:10.1103/PhysRevLett.77.2002. PMID:10061832.
(4) Forrest, J. A.; Mattsson, J. *Phys. Rev. E Stat. Phys. Plasmas Fluids Relat. Interdiscip. Top.* **2000**, *61* (1), R53. PMID: 11046371.
(5) Ellison, C. J.; Torkelson, J. M. *Nat. Mater.* **2003**, *2* (10), 695. doi:10.1038/nmat980. PMID:14502273.
(6) Keddie, J. L.; Jones, R. A. L.; Cory, R. A. *Europhys. Lett.* **1994**, *27* (1), 59. doi:10.1209/0295-5075/27/1/011.
(7) Fukao, K.; Miyamoto, Y. *Phys. Rev. E Stat. Phys. Plasmas Fluids Relat. Interdiscip. Top.* **2000**, *61* (2), 1743. PMID: 11046459.
(8) Rotella, C.; Napolitano, S.; Wübbenhorst, M. *Macromolecules* **2009**, *42* (5), 1415. doi:10.1021/ma8027968.
(9) Shin, K.; Obukhov, S.; Chen, J.-T.; Huh, J.; Hwang, Y.; Mok, S.; Dobriyal, P.; Thiyagarajan, P.; Russell, T. P. *Nat. Mater.* **2007**, *6* (12), 961. doi:10.1038/nmat2031.
(10) Reiter, G.; Hamieh, M.; Damman, P.; Sclavons, S.; Gabriele, S.; Vilmin, T.; Raphaël, E. *Nat. Mater.* **2005**, *4* (10), 754. doi:10.1038/nmat1484. PMID:16184173.
(11) Roth, C. B.; Dutcher, J. R. *Phys. Rev. E Stat. Nonlin. Soft Matter Phys.* **2005**, *72* (2), 021803. PMID:16196593.
(12) Frank, B.; Gast, A. P.; Russel, T. P.; Brown, H. R.; Hawker, C. *Macromolecules* **1996**, *29* (20), 6531. doi:10.1021/ma960749n.

(13) O'Connell, P. A.; McKenna, G. B. *Science* **2005**, *307* (5716), 1760. doi:10.1126/science.1105658. PMID:15774754.
(14) Bodiguel, H.; Fretigny, C. *Phys. Rev. Lett.* **2006**, *97* (26), 266105. doi:10.1103/PhysRevLett.97.266105. PMID: 17280434.
(15) Si, L.; Massa, M. V.; Dalnoki-Veress, K.; Brown, H. R.; Jones, R. A. L. *Phys. Rev. Lett.* **2005**, *94* (12), 127801. doi:10.1103/PhysRevLett.94.127801.
(16) Fakhraai, Z.; Forrest, J. A. *Science* **2008**, *319* (5863), 600. doi:10.1126/science.1151205. PMID:18239120.
(17) Qi, D.; Fakhraai, Z.; Forrest, J. A. *Phys. Rev. Lett.* **2008**, *101* (9), 096101. doi:10.1103/PhysRevLett.101.096101. PMID: 18851624.
(18) Papaléo, R. M.; Leal, R.; Carreira, W. H.; Barbosa, L. G.; Bello, I.; Bulla, A. *Phys. Rev. B* **2006**, *74* (9), 094203. doi:10.1103/PhysRevB.74.094203.
(19) Gasemjit, P.; Johannsmann, D. *J. Polym. Sci., Part B: Polym. Phys.* **2006**, *44* (20), 3031. doi:10.1002/polb.20922.
(20) Winnit, M. A. *Curr. Opin. Colloid Interface Sci.* **1997**, *2*, 192.
(21) Steward, P. A.; Hearn, J.; Wilkinson, M. C. *Adv. Colloid Interface Sci.* **2000**, *86* (3), 195. doi:10.1016/S0001-8686(99) 00037-8. PMID:10997764.
(22) Sasaki, T.; Shimizu, A.; Mourey, T. H.; Thurau, C. T.; Ediger, M. D. *J. Chem. Phys.* **2003**, *119* (16), 8730. doi:10. 1063/1.1613257.
(23) Herminghaus, S.; Seemann, R.; Landfester, K. *Phys. Rev. Lett.* **2004**, *93* (1), 017801. doi:10.1103/PhysRevLett.93. 017801.
(24) Nawaz, Q.; Rharbi, Y. *Macromolcules* **2008**, *41* (15), 5928. doi:10.1021/ma7028049.
(25) Chevalier, Y.; Pichot, C.; Graillat, C.; Joanicot, M.; Wong, K.; Maquet, J.; Lindner, P.; Cabane, B. *Colloid Polym. Sci.* **1992**, *270* (8), 806. doi:10.1007/BF00776153.
(26) Rharbi, Y.; Boué, F.; Joanicot, M.; Cabane, B. *Macromolecules* **1996**, *29* (12), 4346. doi:10.1021/ma951142u.
(27) Rharbi, Y. *Phys. Rev. E Stat. Nonlin. Soft Matter Phys.* **2008**, *77* (3), 031806. PMID:18517413.
(28) Yousfi, M.; Porcar, L.; Lindner, P.; Boué, F.; Rharbi, Y. *Macromolecules* **2009**, *42* (6), 2190. doi:10.1021/ma802734j.
(29) Spiro, J. G.; Yang, J.; Zhang, J. -X.; Winnik, M. A.; Rharbi, Y.; Vavasour, J. D.; Whitmore, M. D.; Jérôme, R. *Macromolecules* **2006**, *39* (20), 7055. doi:10.1021/ma0526037.
(30) Ferry, J. D. *Viscoelestic Properties of Polymers,* 3rd ed.; Wiley: New York, 1980.
(31) Dhinojwala, A.; Wong, G. K.; Torkelson, J. M. *J. Chem. Phys.* **1994**, *100* (8), 6046. doi:10.1063/1.467115.
(32) Goudy, A.; Gee, M. L.; Biggs, S.; Underwood, S. *Langmuir* **1995**, *11* (11), 4454. doi:10.1021/la00011a045.
(33) Pérez, E.; Lang, J. *Langmuir* **2000**, *16* (4), 1874. doi:10. 1021/la990595f.
(34) Pérez, E.; Lang, J. *Macromolecules* **1999**, *32* (5), 1626. doi:10.1021/ma9704121.
(35) Lin, F.; Meier, D. J. *Langmuir* **1996**, *12* (11), 2774. doi:10. 1021/la951554w.
(36) Russel, W. B.; Wu, N.; Man, W. *Langmuir* **2008**, *24* (5), 1721. doi:10.1021/la702633t. PMID:18197713.
(37) Hertz, H. *J. Reine Angew. Math.* **1881**, *92*, 156.
(38) Hertz, H. *Gesammelte Werke* **1895**, *1*, 155.
(39) Lin, Y. H.; *J. Phys. Chem. Br.* **2005**, *109*, 17654.